STYRELSEN FÖR

VINTERSJÖFARTSFORSKNING

WINTER NAVIGATION RESEARCH BOARD

Research Report No 96

Maria Tikanmäki, Aki Kinnunen and Pekka Koskinen

AZIMUTHING THRUSTER ICE LOAD DISTRIBUTION STUDIES

Finnish Transport Safety Agency
Finnish Transport Agency
Finland

Swedish Maritime Administration
Swedish Transport Agency
Sweden

Talvimerenkulun tutkimusraportit — Winter Navigation Research Reports
ISSN 2342-4303
ISBN 978-952-311-221-6

FOREWORD

In this report no 96, the Winter Navigation Research Board presents part 1 of 2 of the results of the research project GUIDANCE2016. A method for creating distributions for loading of the strut of an azimuthing thruster, caused by ice impacts on the thruster body and propeller, was derived. These distributions are used in the fatigue design of azimuthing thrusters.

Model results were compared to the load distribution suggested in the Guidelines to the application of the Finnish-Swedish ice class rules. It was found that the dynamics of the thruster may be important for determining the load distribution. No full-scale results were available for comparison but the shapes of the modelled distributions were reasonable and the results can be used to gain insight into the effect of dynamics on the fatigue design of azimuthing thrusters.

The Winter Navigation Research Board warmly thanks Maria Tikanmäki, Aki Kinnunen and Pekka Koskinen for this report.

Turku

October 2017

Jorma Kämäräinen

Finnish Transport Safety Agency

Tomas Årnell

Swedish Maritime Administration

Markus Karjalainen

Finnish Transport Agency

Stefan Eriksson

Swedish Transport Agency

RESEARCH REPORT

VTT-R-00527-17

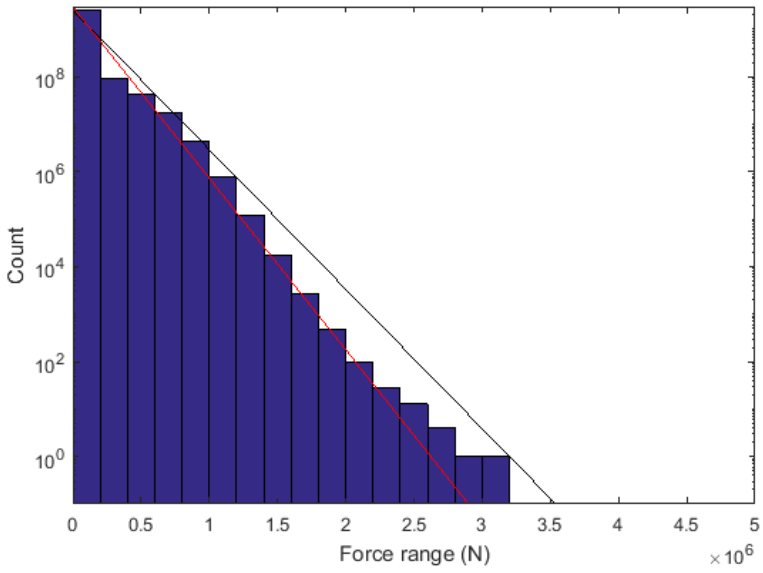

Ice load distributions for azimuthing thrusters

Authors: Maria Tikanmäki, Aki Kinnunen, Pekka Koskinen

Confidentiality: Public

Report's title

Ice load distributions for azimuthing thrusters

Customer, contact person, address	Order reference
Winter Navigation Research Board Jorma Kämäräinen Finnish Transport Safety Agency PO Box 320, FI-00101 Helsinki, Finland	W16-5 GUIDANCE2016
Project name	**Project number/Short name**
GUIDANCE2016	111243 W16-5 GUIDANCE2016
Author(s)	**Pages**
Maria Tikanmäki, Aki Kinnunen, Pekka Koskinen	19/
Keywords	**Report identification code**
azimuthing thruster, ice load, load distribution, extreme value theory	VTT-R-00527-17

Summary

A method to derive ice load distributions for fatigue design of azimuthing thrusters was created. The work was based on the earlier work done for the development of the Finnish-Swedish ice class rules (FSICR).

Load distributions for azimuthing units of four ice-classified ships were calculated with the new method, and the results were then compared with the distributions defined according to suggestion in the guidelines of FSICR. The model results suggested that the effect of dynamics of the thruster might be of importance for defining the ice load range distribution at the thruster strut. Full-scale results were not available for comparison of the results.

Confidentiality	Public

Espoo 30.1.2017

Written by	Reviewed by	Accepted by
Maria Tikanmäki Research Scientist	Pekka Koskinen Senior Specialist	Tuomas Sipilä Research Team Leader

VTT's contact address

P.O. Box 1000, FI-02044 VTT, Finland

Distribution (customer and VTT)

Customer : 1 print + PDF electronic copy
VTT : 2 prints (archive and author) + PDF electronic copy

Contents

1. Introduction

Azimuthing propulsion units experience ice loadings during winter navigation. In the design of azimuthing thrusters, both extreme and fatigue loads need to be taken into account. Extreme loads caused by impact of ice to a hull of an azimuthing thruster (eg. Kinnunen, Koskinen, & Tikanmäki, 2015; Kinnunen, Tikanmäki, & Heinonen, 2016), and ice loads caused by an ice impact to propeller blades have been studied in previous works (eg. Marquis, Koski, & Koskinen, 2008). An extreme load is the load expected to happen once during the design life of the thruster. For the fatigue design of thrusters, the load distribution and number of lower level loadings need to be known.

In this study, a theoretical model to estimate the total ice load distribution for an azimuthing thruster is derived based on the earlier studies and the Finnish-Swedish ice class rules (FSICR) (TraFi & Swedish Transport Agency, 2016a). Ice load distributions are then presented for case studies, and these results are compared to the distribution estimates explained in the guidelines for the application of the FSICR (TraFi & Swedish Transport Agency, 2016b). This comparison reveals applicability of the load distribution estimates for the fatigue design of azimuthing thrusters.

2. Limitations

Basic understanding of the ice load distribution concept is found. This is a primer to the subject not a fully exhaustive research. Full-scale data of ice load distributions for thruster body are not available, and this limits the study to be based on theoretical consideration and expert judgement.

3. Methods

In this study, an ice load distribution for azimuthing thrusters are modelled with Monte Carlo simulation as follows:

1) The total number of loads is calculated as presented in section 3.1, and loads are then divided as impacts to the propeller blades and to the thruster hull.

2) The propeller blade forces are divided as backward and forward bending loads, and calculated as presented in section 3.2. The dynamic magnification of the loads is also taken into account to derive the loads on the thruster hull.

3) Impacts to the thruster hull are calculated as presented in section 3.3.

4) The calculated loads are then combined to form a total distribution of the force range for the lifetime of the thruster as explained in section 3.4.

3.1 The number of ice loads during the design life

In the new version of guidelines for the application of the FSICR (TraFi & Swedish Transport Agency, 2016b), it is recommended that the total number of ice loads for the whole thruster N_t is taken as

$$N_t = Z \cdot N_{ice} \cdot C_{nice} \tag{1.1}$$

where Z is the number of blades, N_{ice} is the number of blade loading defined below, and C_{nice} is a factor taking into account the thruster body loads on top of the propeller induced loads. Guidelines suggest that if C_{nice} is not known, a value of 1.2 should be used. We adopt this formula for the number of ice loads with C_{nice} estimated from the geometry of the thruster as follows.

If the probability of impact with an ice block is assumed to be uniform over the whole area of the longitudinal cross section of the thruster, the value of C_{nice} can be estimated for an open propeller by

$$C_{nice} = 1 + \frac{A_1}{n_b A_2} = 1 + \frac{\left(d_{h,p} / D\right)^2}{n_b \left(1 - \left(d_{h,p} / D\right)^2\right)} \tag{1.2}$$

where A_1 is the area of the thruster hub, A_2 is the area where blades sweep, n_b is the average amount of blade hits per an ice block, $d_{h,p}$ is the hub diameter for pulling propeller and the pod diameter for pushing propeller, and D is the propeller diameter.

The same can be estimated for a ducted propeller as follows

$$C_{nice} = 1 + \frac{A_1}{n_b A_2} = 1 + \frac{{d_{h,p}}^2 + 4Dh_n + 4{h_n}^2}{n_b \left(D^2 - {d_{h,p}}^2\right)} \tag{1.3}$$

where h_n is the thickness of the nozzle. Schematic cross sections of both open and ducted propellers are shown in Figure 1.

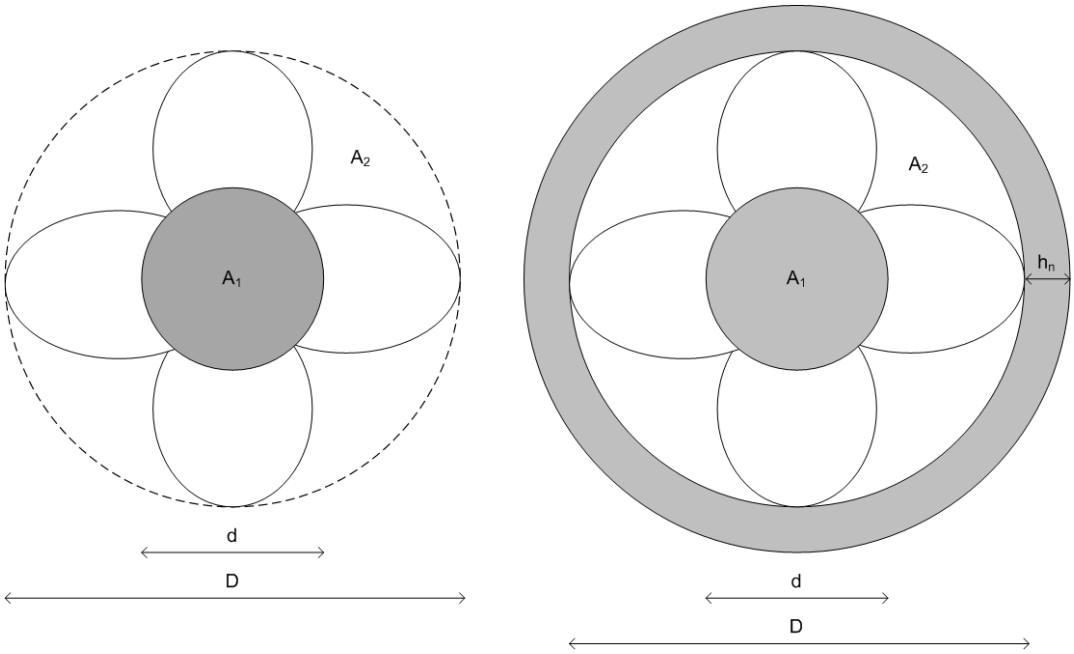

Figure 1. Schematic cross-sections of open (left) and ducted propeller (right). The grey area shows the places where ice impact is delivered straight to the thruster hull structure and the white area shows the area where ice impacts to blades.

Number of ice impacts N_{ice} is defined in the suggested new version of the FSICR (TraFi & Swedish Transport Agency, 2016a) as

$$N_{ice} = k_1 k_2 k_3 N_{class} n \tag{1.4}$$

where k_1 is the propeller location factor shown in Table 1, k_2 the submersion factor, k_3 is the propulsion type factor shown in Table 2, N_{class} is a reference number of loads for ice classes shown in Table 3, and n is the nominal rotational speed.

Table 1. Propeller location factor k_1.

Centre propeller Bow first operation		Wing propeller Bow first operation	Pulling propeller (wing and centre) Bow propeller or Stern first operation
k_1	1	2	3

Table 2. Propulsion type factor k_3.

type	fixed	azimuthing
k_3	1	1.2

Table 3. Reference number of loads for ice classes N_{class}.

Class	IA Super	IA	IB	IC
impacts in life/*n*	$9 \cdot 10^6$	$6 \cdot 10^6$	$3.4 \cdot 10^6$	$2.1 \cdot 10^6$

The submersion factor k_2 is determined from the equation

$$\begin{aligned} k_2 &= 0.8 - f && \text{when} \quad f < 0 \\ &= 0.8 - 0.4 \cdot f && \text{when} \quad 0 \le f \le 1 \\ &= 0.6 - 0.2 \cdot f && \text{when} \quad 1 < f \le 2.5 \\ &= 0.1 && \text{when} \quad f > 2.5 \end{aligned} \tag{1.5}$$

where the immersion function f is

$$f = \frac{h_o - H_{ice}}{D/2} - 1 \tag{1.6}$$

where h_o is the depth of the propeller centreline at the lower ice waterline (LIWL) of the ship, and H_{ice} is the thickness of the design maximum ice block entering the propeller.

Table 4. The thickness of the design maximum ice block entering the propeller for each ice class.

	IA Super	IA	IB	IC
Thickness of the design maximum ice block entering the propeller (H_{ice})	1.75 m	1.5 m	1.2 m	1.0 m

3.2 Load distributions for blade loads

The load distribution for blade loads is defined as follows:

1) The maximum blade bending forces are first calculated as presented in the section 3.2.1 for open propellers and in the section 3.2.2 for ducted propellers.

2) The loads for the Monte-Carlo simulation are then drawn from the distribution of blade loads presented in the section 3.2.3.

3) Dynamic magnification of these loads is then calculated as presented in the section 3.2.4

3.2.1 Maximum blade bending forces for open propellers

For open propellers, the maximum backward blade force F_b is taken as

$$\begin{aligned} F_b &= 27 \cdot [n \cdot D]^{0.7} \cdot \left[\frac{EAR}{Z}\right]^{0.3} \cdot D^2 \text{ [kN], when } D \le D_{\text{limit}} \\ F_b &= 23 \cdot [n \cdot D]^{0.7} \cdot \left[\frac{EAR}{Z}\right]^{0.3} \cdot D \cdot H_{ice}{}^{1.4} \text{ [kN], when } D > D_{\text{limit}} \end{aligned} \tag{1.7}$$

where $D_{limit} = 0.85 \cdot H_{ice}{}^{1.4}$, n is the nominal rotational speed (at MCR in free running condition) for a CP propeller and 85% of the nominal rotational speed (at MCR in free running condition for a FP propeller. Further, the maximum forward blade force F_f for open propellers is taken as

$$\begin{aligned} F_f &= 250 \cdot \left[\frac{EAR}{Z}\right] \cdot D^2 \text{ [kN], when } D \le D_{\text{limit}} \\ F_f &= 500 \cdot \left[\frac{EAR}{Z}\right] \cdot D \cdot \frac{1}{\left(1 - \frac{d}{D}\right)} \cdot H_{ice} \text{ [kN], when } D > D_{\text{limit}} \end{aligned} \tag{1.8}$$

where $D_{limit} = \dfrac{2}{\left(1 - \dfrac{d}{D}\right)} \cdot H_{ice}$. (TraFi & Swedish Transport Agency, 2016a)

3.2.2 Maximum blade bending forces for ducted propellers

For ducted propellers, the maximum backward blade force F_b is defined as

$$\begin{aligned} F_b &= 9.5 \cdot [n \cdot D]^{0.7} \cdot \left[\frac{EAR}{Z}\right]^{0.3} \cdot D^2 \text{ [kN], when } D \le D_{\text{limit}} \\ F_b &= 66 \cdot [n \cdot D]^{0.7} \cdot \left[\frac{EAR}{Z}\right]^{0.3} \cdot D^{0.6} \cdot H_{ice}{}^{1.4} \text{ [kN], when } D > D_{\text{limit}} \end{aligned} \tag{1.9}$$

where $D_{limit} = 4 \cdot H_{ice}$, and the maximum forward blade ice force F_f for ducted propellers

$$F_f = 250 \cdot \left[\frac{EAR}{Z}\right] \cdot D^2 \text{ [kN], when } D \le D_{\text{limit}}$$
$$F_f = 500 \cdot \left[\frac{EAR}{Z}\right] \cdot D \cdot \frac{1}{\left(1 - \frac{d}{D}\right)} \cdot H_{ice} \text{ [kN], when } D > D_{\text{limit}} \quad (1.10)$$

where $D_{limit} = \frac{2}{\left(1 - \frac{d}{D}\right)} \cdot H_{ice}$. (TraFi & Swedish Transport Agency, 2016a)

3.2.3 Distribution of blade loads

The probability distributions of blade loads have been studied before by Marquis et al. (2008). Their findings are based on the long-term measurements of blade loads on m/s Gudingen (Koskinen & Jussila, 1991) and adopted for the FSICR (TraFi & Swedish Transport Agency, 2016a). The Weibull-type distribution of ice loads for blades is defined by

$$P\left(\frac{F_{ice}}{F_{ice,\max}} \ge \frac{F}{F_{ice,\max}}\right) = e^{\left(-\left(\frac{F}{F_{ice,\max}}\right)^k \cdot \ln(N)\right)} \quad (1.11)$$

where $F_{ice,\max}$ is the maximum ice load effecting on blades, k is the shape parameter, and F_{ice} is the random variable for ice loads on the blade defined as $0 \le F_{ice} \le F_{ice,\max}$. The shape parameter k is 0.75 for open and 1.0 for ducted propellers.

In this study, it is assumed that 80 % of the ice loads are bending blades forwards and 20 % backwards. For the Monte-Carlo simulation of the total loads, loads are thus drawn from the above distribution with $F_{ice,\max} = F_f$ and $N = 0.8Z \cdot N_{ice}$ for the forward bending loads, and $F_{ice,\max} = F_b$ and $N = 0.2Z \cdot N_{ice}$ for the backward bending loads.

3.2.4 Dynamic magnification of blade loads

Since the actual goal is to define ice load distributions on the thruster hull, the dynamic excitation has to be taken into account to see how blade loads affect the thruster hull. The axial sinusoidal extreme excitation for any direction is taken as

$$F_{bla}(\varphi) = F_{bla} C_{q1} \sin(Z\varphi + \alpha_1) \text{ [kN]} \quad (1.12)$$

where F_{bla} is the maximum of backward F_b and forward blade load F_f, C_{q1} is the first blade order Fourier component, φ is the angle of rotation, and α_1 is the first order phase angle of excitation component. Here, we only need to take into account the maximum, and thus

$$F_{bla,\max} = F_{bla} C_{q1} \text{ [kN]} \quad (1.13)$$

where C_{q1} is 0.375 for three-blade propellers and 0.36 if there are more than three blades.

The actual axial response force is then defined by

$$F_{bla,resp,\max} = C_{DM} F_{bla,\max} \ [\text{kN}] \tag{1.14}$$

where C_{DM} is the dynamic magnification factor. (TraFi & Swedish Transport Agency, 2016a)

The dynamic magnification factor is ship and thruster dependent and is a function of the used power. In order to estimate the ice load distribution, the dynamic magnification factor distribution needs to be estimated.

Three different dynamic magnification factor distributions are defined in Table 5. The different distributions are used when a) no dynamic magnification is present (C_{DM1}), b) dynamic magnification is at intermediate power levels (C_{DM2}, "typical scenario"), and c) dynamic magnification is at high power levels (C_{DM3}, "a worst-case scenario").

Table 5. The percentage of forward and backward bending loads and three different distributions of the dynamic magnification factors at each power class.

Power (% of maximum)	Percentage of forward bending loads in each power class (%)	Percentage of backward bending loads in each power class (%)	C_{DM1}	C_{DM2}	C_{DM3}
0-10	0	0	1	1	1
10-20	2	30	1	1	1
20-30	2	30	1	1	1
30-40	2	20	1	1	1
40-50	2	10	1	1	1
50-60	2	2	1	1	1
60-70	10	2	1	5	1
70-80	20	2	1	1	1
80-90	30	2	1	1	1
90-100	30	2	1	1	5

3.3 Impacts to the thruster hull

Direct impacts to the thruster hull are estimated by the formula derived for the Finnish-Swedish ice class rules (TraFi & Swedish Transport Agency, 2016a). The formula is a simplification of the ice impact calculation method which is verified by experiments (Kinnunen et al., 2015). The ice impact load is defined as

$$F_{ti} = C_{DMI} 34.5 R_c^{0.5} (m_{ice} v_s^2)^{0.333} \text{ [kN]} \quad (1.15)$$

where R_c is the impacting sphere radius [m], m_{ice} is the ice block mass [kg], v_s is the ship speed at the time of contact [m/s], and C_{DMI} is the dynamic magnification factor for impact loads taken as 1.0 for class IC, 1.1 for class IB, 1.2 for class IA, 1.3 for class IA Super if not known.

Here, for determining the ice block size distribution, we adopt a lognormal distribution for the length of the ice blocks at a broken channel with a cumulative distribution function as

$$F(l) = \frac{1}{2} + \frac{1}{2} \text{erf}\left(\frac{\ln l - \mu}{\sqrt{2}\sigma} \right) \quad (1.16)$$

where $\mu = -0.563$ and $\sigma = 0.358$ as proposed by Tuovinen (1979). The mass of the ice block is then calculated by

$$m = l^2 h \rho \quad (1.17)$$

where ρ is the density of ice, and h is the thickness of ice defined to give extreme impacting ice mass on average once in a lifetime of the thruster. As defined in FSICR, this extreme ice mass for 1AS is 8670kg, for 1A 5460 kg, for 1B 2800 kg, and for 1C 1600 kg. For 1AS, h is roughly 0.5 m. The actual value depends on the total number of loads which depends on the type of the thruster.

The distribution of ice impact loads to the thruster hull is then derived by Monte-Carlo simulation, where the length of an ice block is drawn from the distribution defined in equation (1.16), and the speed is drawn from a uniform distribution between 0 and 12 knots.

3.4 Total load distribution

The total outcome of the study is a distribution of a load range. For this distribution the impact loads for hull are taken as such and loads caused by impacts to blades are multiplied by factor 2.

4. Results

The distributions of load ranges were calculated for four example ships. Main parameters of the thrusters are shown in Table 6.

Table 6. Main variables of thrusters of example ships 1, 2, 3, and 4.

	Ship 1	Ship 2	Ship 3	Ship 4
Type of the propulsion unit	Ducted	Open	Open	Open
Ice class	1AS	1AS	1AS	1C
Propeller diameter D	4.2	5.7	4.2	3.8
Hub diameter d	1.5	1.7	1.5	1.6
Number of blades Z	4	4	4	4
Total number of ice loads N_t	$2.0 \cdot 10^9$	$1.8 \cdot 10^9$	$2.5 \cdot 10^9$	$3.7 \cdot 10^7$

The distributions of load ranges for the example ships are shown below from Figure 2 to Figure 10 with three different dynamic magnification distributions. The first figure for each ship presents the distribution without any dynamic magnification of blade loads. The second one presents the distribution with dynamic magnification being at intermediate power levels resembling typical design. The third figure for each ship presents the worst case scenario where the highest dynamic magnification is achieved with full power usage.

In these figures, bars show the amount of force ranges larger or equal to the corresponding value. Black curves are Weibull-type distributions defined in equation (1.11) multiplied by total number of ice loads N_t. The distribution has a shape factor 1, the maximum ice load, and the number of loads taken from the model results. The red curve is again Weibull-type distribution with a shape factor 1 but the value for the maximum ice load is taken as the maximum of the longitudinal extreme impact load and the longitudinal extreme ridge interaction load as defined in the guidelines of FSICR, and the number of loads is taken from the equation (1.1) with C_{nice} being 1.2 as suggested in the guidelines of FSICR.

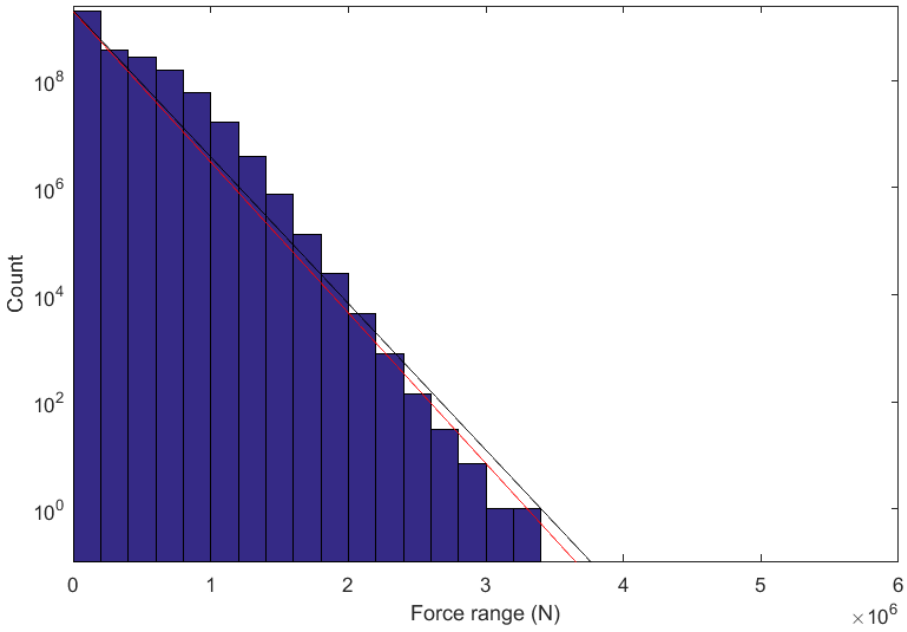

Figure 2. The modelled force ranges at the thruster strut for ship 1 without any dynamic magnification of blade loads (C_{DM1} in Table 5 used). The black curve is Weibull distribution with a shape factor 1, and the maximum ice load and the number of loads are taken from the model results. The red curve is Weibull distribution with the values taken from the guidelines of FSICR.

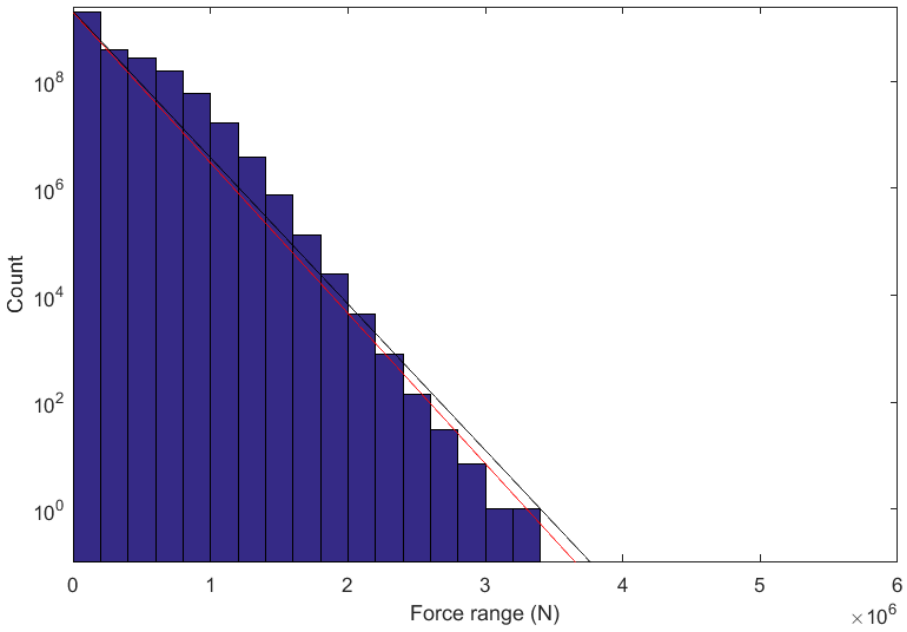

Figure 3. The modelled force ranges at the thruster strut for ship 1 with dynamic magnification of blade loads at intermediate power levels (C_{DM2} in Table 5 used The black curve is Weibull distribution with a shape factor 1, and the maximum ice load and the number of loads are taken from the model results. The red curve is Weibull distribution with the values taken from the guidelines of FSICR.

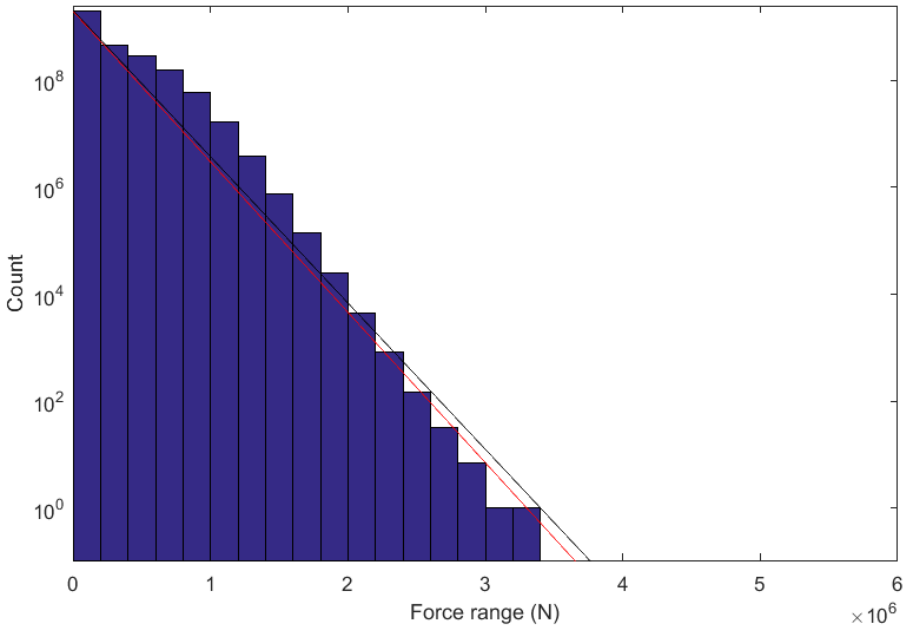

Figure 4. The modelled force ranges at the thruster strut for ship 1 with dynamic magnification of blade loads at high power levels (C_{DM3} in Table 5 used). The black curve is Weibull distribution with a shape factor 1, and the maximum ice load and the number of loads are taken from the model results. The red curve is Weibull distribution with the values taken from the guidelines of FSICR.

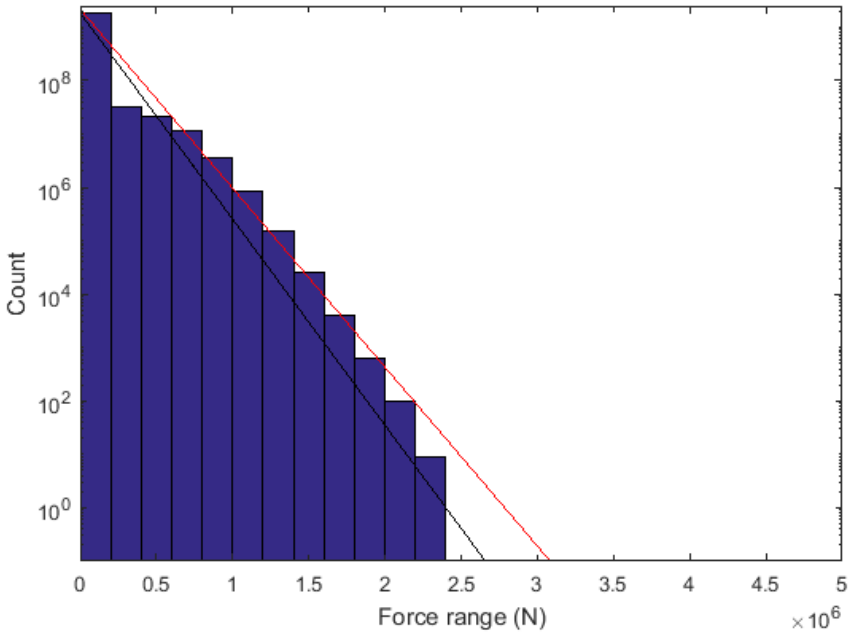

Figure 5. The modelled force ranges at the thruster strut for ship 2 without any dynamic magnification of blade loads (C_{DM1} in Table 5 used). The black curve is Weibull distribution with a shape factor 1, and the maximum ice load and the number of loads are taken from the model results. The red curve is Weibull distribution with the values taken from the guidelines of FSICR.

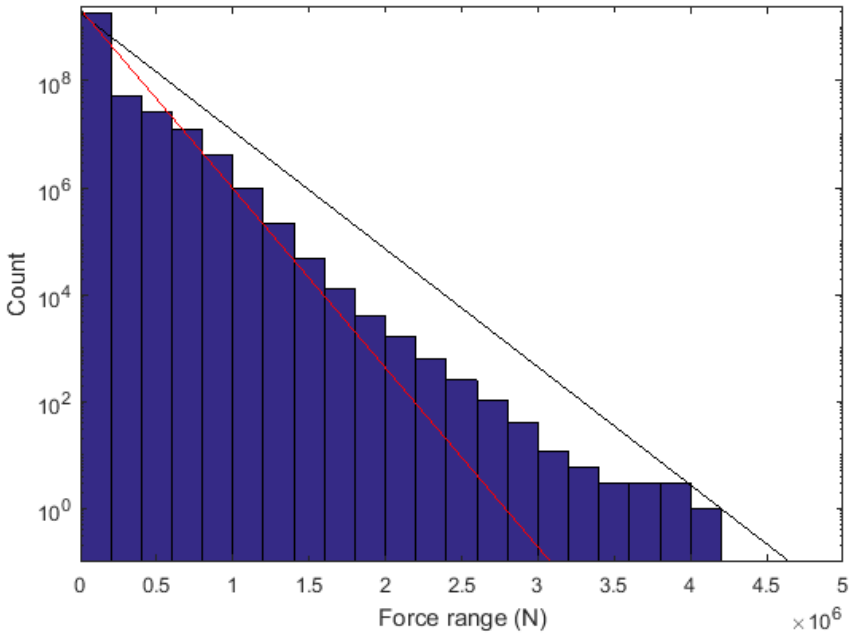

Figure 6. The modelled force ranges at the thruster strut for ship 2 with dynamic magnification of blade loads at intermediate power levels (C_{DM2} in Table 5 used). The black curve is Weibull distribution with a shape factor 1, and the maximum ice load and the number of loads are taken from the model results. The red curve is Weibull distribution with the values taken from the guidelines of FSICR.

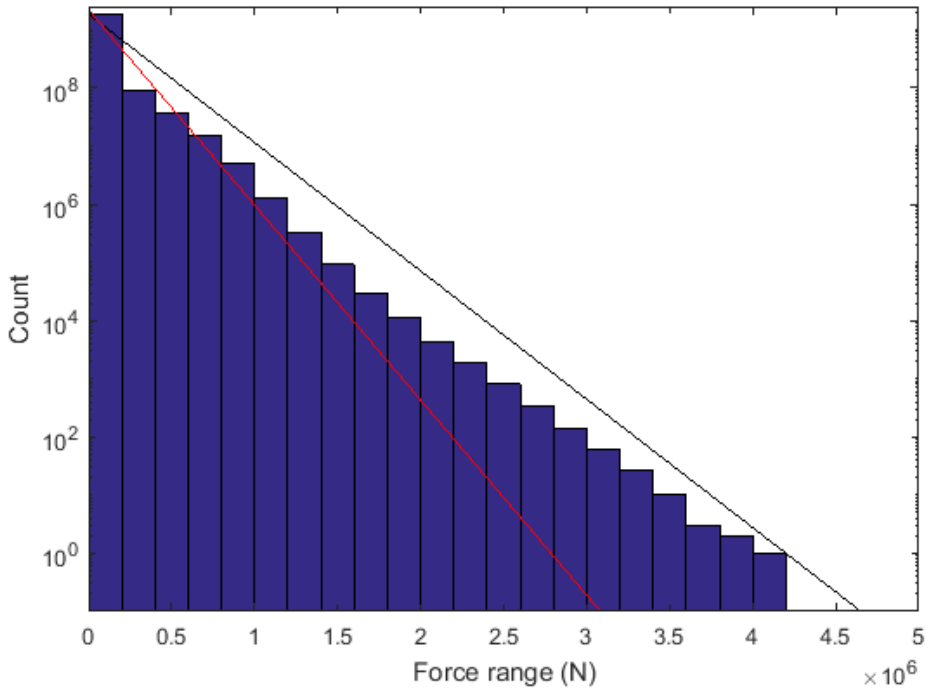

Figure 7. The modelled force ranges at the thruster strut for ship 2 with dynamic magnification of blade loads at high power levels (C_{DM3} in Table 5 used). The black curve is Weibull distribution with a shape factor 1, and the maximum ice load and the number of loads are taken from the model results. The red curve is Weibull distribution with the values taken from the guidelines of FSICR.

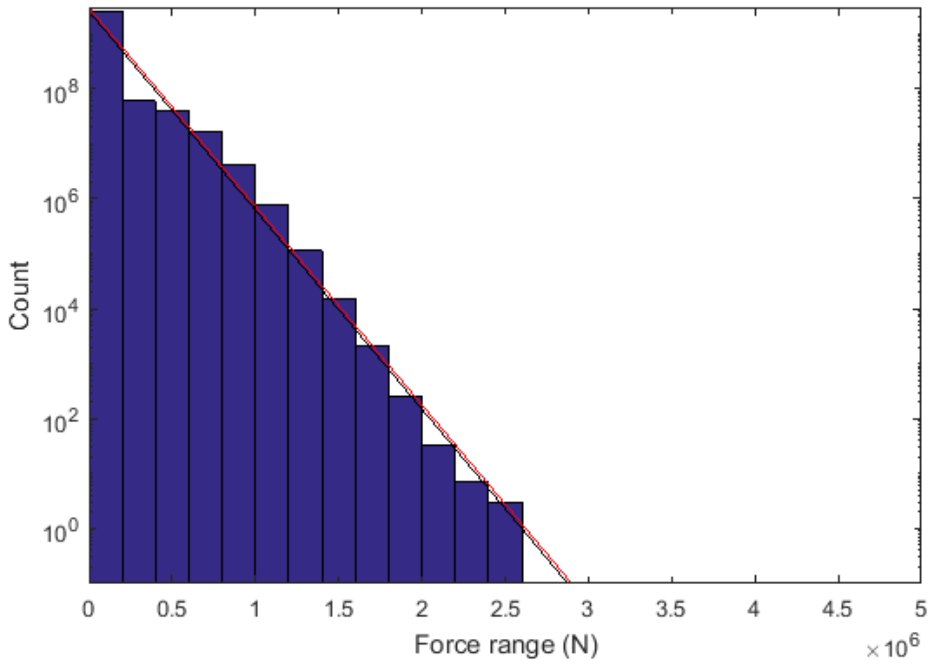

Figure 8. The modelled force ranges at the thruster strut for ship 3 without any dynamic magnification of blade loads (C_{DM1} in Table 5 used). The black curve is Weibull distribution with a shape factor 1, and the maximum ice load and the number of loads are taken from the model results. The red curve is Weibull distribution with the values taken from the guidelines of FSICR.

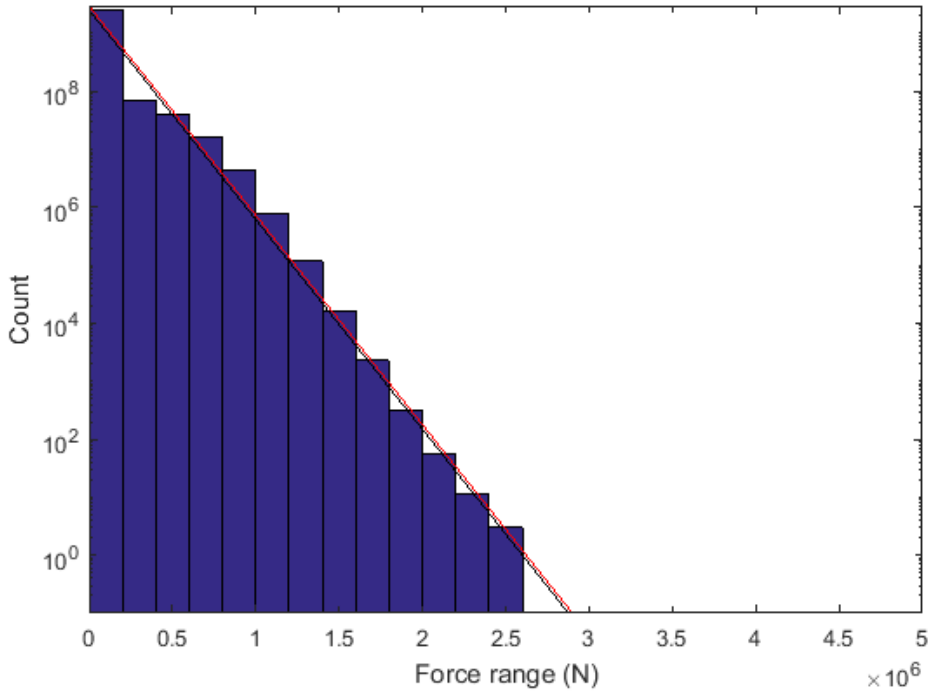

Figure 9. The modelled force ranges at the thruster strut for ship 3 with dynamic magnification of blade loads at intermediate power levels (C_{DM2} in Table 5 used). The black curve is Weibull distribution with a shape factor 1, and the maximum ice load and the number of loads are taken from the model results. The red curve is Weibull distribution with the values taken from the guidelines of FSICR.

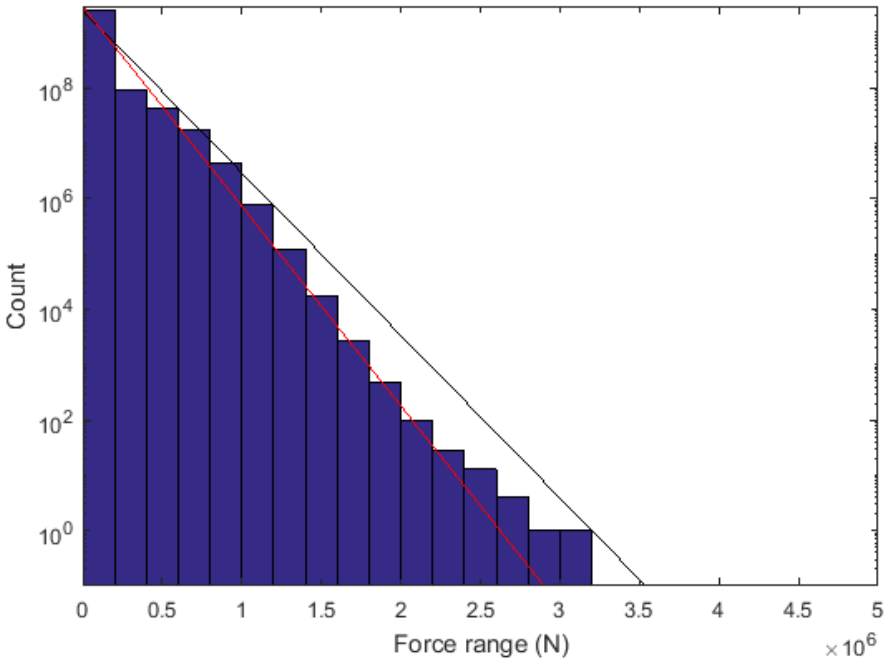

Figure 10. The modelled force ranges at the thruster strut for ship 3 with dynamic magnification of blade loads at high power levels (C_{DM3} in Table 5 used). The black curve is Weibull distribution with a shape factor 1, and the maximum ice load and the number of loads are taken from the model results. The red curve is Weibull distribution with the values taken from the guidelines of FSICR

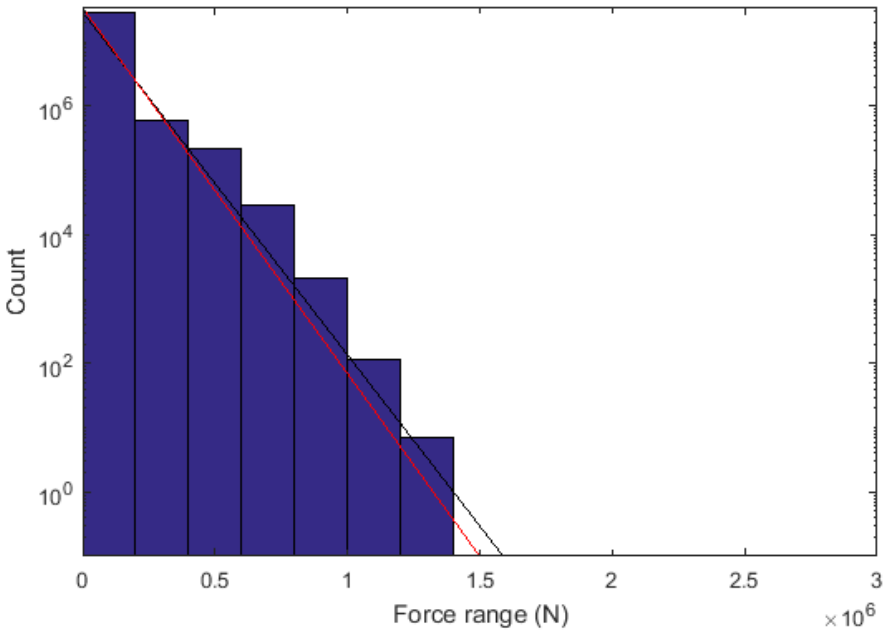

Figure 11. The modelled force ranges at the thruster strut for ship 4 without any dynamic magnification of blade loads (C_{DM1} in Table 5 used). The black curve is Weibull distribution with a shape factor 1, and the maximum ice load and the number of loads are taken from the model results. The red curve is Weibull distribution with the values taken from the guidelines of FSICR.

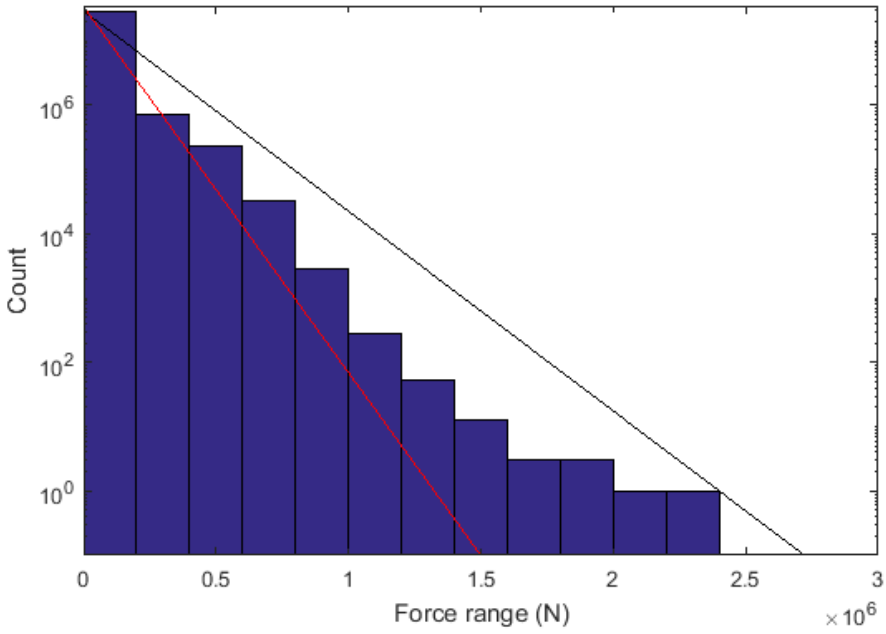

Figure 12. The modelled force ranges at the thruster strut for ship 4 with dynamic magnification of blade loads at intermediate power levels (C_{DM2} in Table 5 used). The black curve is Weibull distribution with a shape factor 1, and the maximum ice load and the number of loads are taken from the model results. The red curve is Weibull distribution with the values taken from the guidelines of FSICR.

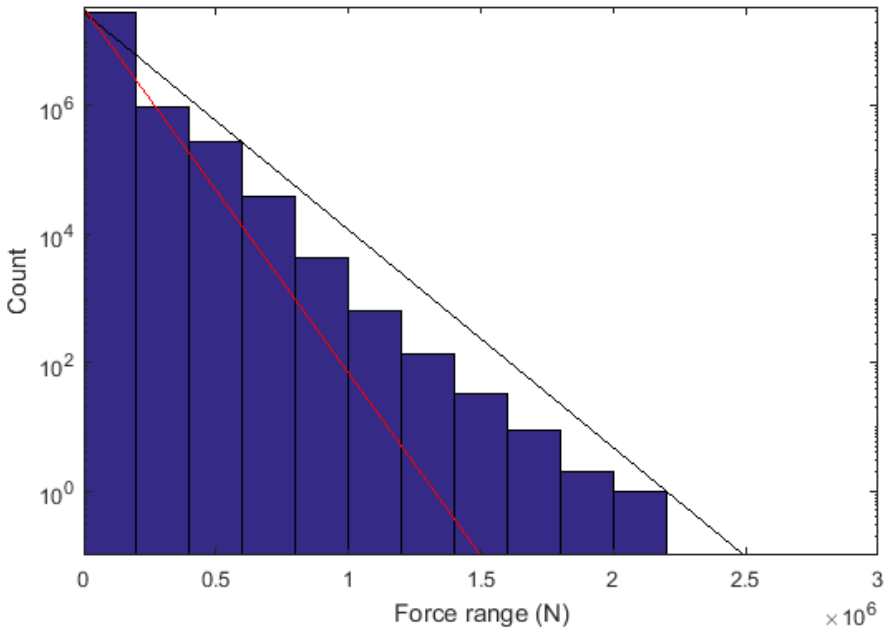

Figure 13. The modelled force ranges at the thruster strut for ship 4 with dynamic magnification of blade loads at high power levels (C_{DM3} in Table 5 used). The black curve is Weibull distribution with a shape factor 1, and the maximum ice load and the number of loads are taken from the model results. The red curve is Weibull distribution with the values taken from the guidelines of FSICR.

5. Conclusions

In general, it was noted that the ice hitting the thruster body caused most severe contact loads. However, in some cases the blade loads caused more severe response load ranges at the thruster strut after the dynamic magnification was taken into account. It can be noted that if the dynamic magnification factor at the resonance is higher than 5 it can cause even higher response load ranges. The dynamic magnification factor and the power levels when resonance is achieved are thruster-dependent and are given as examples in this study. The results suggest that the dynamic magnification might be of importance in the fatigue design of a thruster.

In the guidelines for the application of the Finnish-Swedish ice class rules (TraFi & Swedish Transport Agency, 2016b), a Weibull-type load distribution (eq. (1.11)) with a shape factor 1 is suggested for total loads if no proven method exists. It is also suggested that the maximum ice load $F_{ice,\max}$ is taken as a maximum of the extreme ridge load and the extreme ice impact load defined in the FSICR ice class rules. The results achieved without dynamic magnification suggest that this method is reasonable. When dynamics of the thruster are taken into account as described above, the suggested distribution might underestimate load ranges at the thruster strut. In that case, dynamically magnified blade loads should be taken into account when defining the maximum ice force $F_{ice,\max}$ for the distribution function.

The estimation method presented above involves assumptions about the distributions of the vessel operation speed, the ice block size, the vessel operation power, the dynamic magnification factor, and the load type vs. power. Most of these are vessel-dependent, and the ice block size distribution is not well known. Thus, these distributions need to be estimated. Since no available full-scale data of the thruster hull loads exists, the validity of assumptions cannot be evaluated in detail. From the expert point of view, the shapes of the modelled distributions seem to be reasonable, and thus the examples presented here can be used to gain insight of the effect of the dynamics for the fatigue design of the thruster.

6. Summary

A method to derive ice load distributions for fatigue design of azimuthing thrusters was created. The work was based on the earlier work done for the development of the Finnish-Swedish ice class rules (FSICR).

Load distributions for azimuthing units of four ice-classified ships were calculated with the new method, and the results were then compared with the distributions defined according to suggestion in the guidelines of FSICR. The model results suggested that the effect of dynamics of the thruster might be of importance for defining the ice load range distribution at the thruster strut. Full-scale results were not available for comparison of the results.

Acknowledgements

This work was funded by the Winter Navigation Research Board which is gratefully acknowledged.

References

Kinnunen, A., Koskinen, P., & Tikanmäki, M. (2015). Ice-structure impact contact load calculation with dynamic model and simplified load formula. In *Proceedings of the 23rd International Conference on Port and Ocean Engineering under Arctic Conditions*. June

14-18, 2015 Trondheim, Norway.

Kinnunen, A., Tikanmäki, M., & Heinonen, J. (2016). An energy model for ice crushing in ice-structure impact. In *Proceedings of the 23rd IAHR International Symposium on Ice*. Ann Arbor, Michigan, USA.

Koskinen, P., & Jussila, M. (1991). *Potkurin lavan jääkuormien pitkäaikaismittaus m/s Gudingenilla*. *VTT Technical Research Centre of Finland, Research Notes 1260 (in Finnish)*. Espoo, Finland.

Marquis, G., Koski, K., & Koskinen, P. (2008). Fatigue design methodology for propellers operating in ice (Rev2). *VTT Technical Research Centre of Finland*, *VTT-R-0071*, 23.

TraFi, & Swedish Transport Agency. (2016a). *New version of FSICR 2010 – 25 August 2016*.

TraFi, & Swedish Transport Agency. (2016b). *New version of the guidelines for the application of the Finnish-Swedish ice class rules – 25 August 2016*.

Tuovinen, P. (1979). *The size distribution of ice blocks in a broken channel*. *Helsinki University of Technology, Ship hydrodynamics laboratory*.